Double Trellis-Coded CPM

Weiling LIU Johannes HUBER

University of the Federal Armed Forces Munich
Institute for Communication Engineering
D - 8014 Neubiberg, FRG

ABSTRACT

The method of multiple trellis-coded modulation is applied to continuous phase modulation (CPM). Especially double trellis-coded quaternary CPM schemes using convolutional codes with an effective rate 2/4 are considered. Tables of optimum codes and minimum Euclidean distances are given for several frequency impulses and numbers of trellis branches per symbol interval, which have to be processed by a Viterbi-decoder. The results are clearly superior to single trellis-coded schemes with rate 1/2 codes. These improvements are accomplished by a proper selection of double channel symbols. Additionally this method offers improved receiver implementation properties. For a further reduction of complexity a modified decision feedback sequence estimation is proposed.

I. INTRODUCTION

This paper deals with the combination of convolutional codes and continuous phase modulation (CPM |1,2|) in such way that each codeword is mapped to the signal within two adjacent modulation time intervals. In the sense of trellis-codes |3| the redundancy is transmitted by means of an increased signal space. Refering to |4| we call such schemes "double trellis-coded CPM". The expression "multidimensional" |3,5| will not be used for CPM, because the set of all signals within one modulation time interval (the elements of the signal set) already form a multidimensional signal space.

Very sophisticated codes, offering high theoretical coding gains at the prize of very expensive decoders, are not the object of this paper, but methods, with which considerable gains can be achieved by short codes, and therefore allow the realization of a Viterbi-decoder at high data rates. The first method is a special (redundant) mapping rule, which implicates a reduction of the number of different memory states of the modulation process. In some cases a state reduction similar to |6| is possible by a proper coordination of both memories, within the encoder and the modulation process. Additionally, it will be shown that the decoding effort may be halved by the application of a modified Decision-Feedback-Sequence-Estimation (cf.|7,8|) instead of Maximum-Likelihood-Sequence-Estimation without noteworthy losses.

The realization expense of a Viterbi-decoder applied to multiple trellis-coded schemes cannot be estimated simply by the number $Z = 2^{\nu}$ of different encoder-modulation states. A better index is the average number of trellis branches, which have to be processed per modulation interval (|3|). For k binary encoder inputs per modulation interval T and a κ-fold multiple trellis-coded scheme (- the signal of κ intervals regarded as one channel symbol -), this number is given by:

$$A = 2^{a}; \quad a = \kappa k + \nu - \mathrm{ld}\,\kappa \qquad (1)$$

This exponent a of the normalized number of branches (ENNB) indicates that an increase of the constraint length within the coded signal by κ-fold multiple trellis-codes causes a comparable expense as an increase by a long convolutional code. Only for k = 1 double trellis-coded schemes ($\kappa = 2$) have the identical ENNB $a = \nu+1$ as single trellis-codes with the same number of states. Therefore mainly short codes with an effective rate 2/4 ($\kappa = 2$) are considered and compared with rate 1/2 codes ($\kappa = 1$), both combined with quaternary CPM.

II. REDUNDANT MAPPING WITH STATE REDUCTION

Similar to |6| M-ary CPM is interpreted as a naturally trellis-coded scheme with $M^{L} \cdot q$ different signal-elements within one modulation interval T (L,q denoting the duration of the frequency impulses and the denominator of the rational modulation index h = p/q (p and q no common divisor cf.|1,2,6|), respectively). A CPM modulator may be divided into a redundant encoder, which contains the inherent memory of the modulation process and a table of all signal-elements. The signal-element for the time interval $(m-1)T \leq t < mT$ may be addressed by the last L phase-increments

CH2538-7/88/0000-1692 $1.00

$\alpha_{m-i} \in \{\pm1, \pm3, .., \pm(M-1)\}$; $i \in \{0, 1, ..., (L-1)\}$, which influence the actual phase-function (intersymbol-interference (ISI) of the frequency impulses) and the phase-state

$$\theta_{m-L} = 2\pi h \left(\left(p \cdot \sum_{i=-\infty}^{m-L} (\alpha_i + M-1)/2 \right) \bmod q \right). \quad (2)$$

The phase-state contains the contribution of frequency impulses to the phase function, which have already completely entered the modulator. The definition (2) of phase-states is valid for a phase measurement according to a reference phase, which differs from the carrier phase (cf.|6|). With this definition the sequences of phase-states form an ergodic Markov chain with q states.

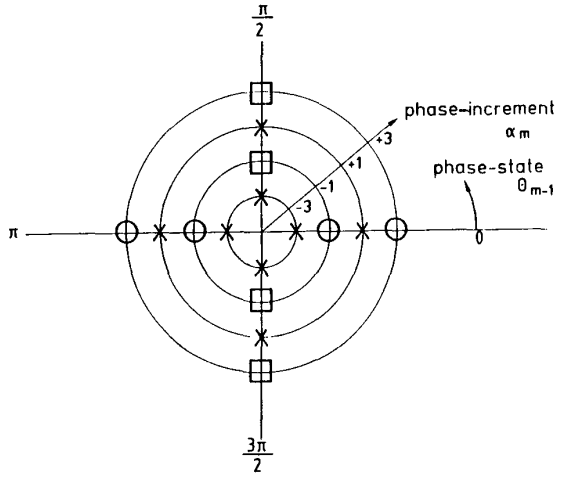

Fig. 1 16 signal-elements of CPM with M=4, h=1/4, L=1, characterized by its phase-state θ_{m-1} and phase-increment α_m

In Fig. 1 all 16 signal-elements of quaternary CPM (M=4) with a modulation index h = 1/4 and L = 1, are represented by points in polar coordinates, in which the phase-state θ_{m-1} determines the angle and the phase-increment α_m the magnitude.

Throughout this paper a mapping of the information to the phase-increment α (phase difference- or frequency-mapping) is provided for the purpose of phase rotational invariance (|6|).

For $M = 2^n$ n binary digits y_j are related to the M-ary phase-increments α (natural mapping):

$$\alpha = \sum_{j=o}^{n-1} y_j \, 2^{j+1} - (M-1) \quad (3)$$

y_o is associated with a phase-increment of $\pm\pi h$, y_1 with $\pm 2\pi h$ etc. Thus, using a $\kappa = c \cdot 2^{\mu}$-fold redundant mapper ($\mu, c \in \mathbb{N}; \mu \leq n$), which guaranties a constant symbol y_o over 2^{μ} modulation intervals T, a constant symbol y_1 over $2^{\mu-1}$ intervals T etc., all the modulator input symbols

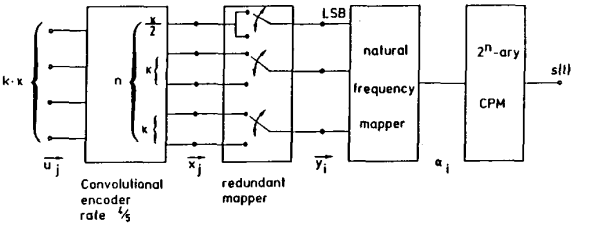

Fig. 2 Block diagram of the κ-fold trellis-coded CPM schemes with redundant mapper

y_l, $l \in \{0,1,.., \mu\}$ generate total phase-increments over one coding interval κT, which are multiples of $2^{\mu} \cdot \pi h$. If the denominator q of the modulation index is divisible by 2^{μ}, the number of possible phase-states at the boundaries of the coding intervals is reduced by the factor 2^{μ} (see eq.(2)). For such a redundant mapper a rate R_m

$$R_m = \left((n-\mu)\kappa + \kappa \sum_{j=1}^{\mu} 2^{-j} \right) / (\kappa \cdot n) = (n-\mu+1-2^{-\mu})/n \quad (4)$$

may be defined.

The number of states and the ENNB are decreased by the redundancy of this mapping method at the prize of bandwidth and squared Euclidean distance normalized to the energy per bit. This is only a good choice, if the expense is more than compensated by a convolutional code with a rate $R_c = k/(n \cdot R_m)$ and a number of states, which is $c \cdot 2^{\mu}$ times greater than that of a comparable code with rate κk/κn. Multiple trellis-coded schemes with a small decoding effort only can be constructed by means of such a redundant mapping method.

III. DOUBLE TRELLIS-CODED QUATERNARY CPM COMBINED WITH RATE 2/3 CODES

In Fig. 3 the phase-state-trellis of 4-ary CPM with modulation index h = 1/4 combined with a redundant mapper for two modulation intervals (κ=2) and a state reduction by a factor 2 (μ=1) is shown. As two phase-states exist at the boundaries of the coding interval 2T, this scheme may be interpreted as an 8-ary extension of MSK. All three binary mapper input symbols cause phase-increments ±π/2 within 2T. Therefore an extraction of the natural trellis-encoder of this scheme gives the circuit shown in Fig. 4, which is linear in the finite field GF(2) and has the identical memory structure as the natural encoder of MSK.

For L=1 only 16 out of all 64 signal-elements over 2T with phase continuity are addressed. Within one interval T only those 12 out of the 16 signal-elements shown in Fig. 1 are used, which are marked by the signs "o" and "x". The signal-elements characterized by "o" are those

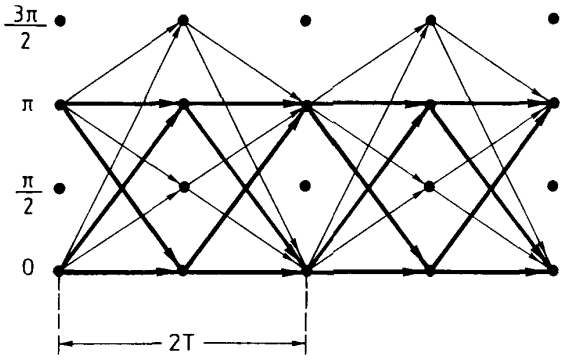

Fig. 3 The phase-state trellis for M=4, h=1/4, κ=2, μ=1

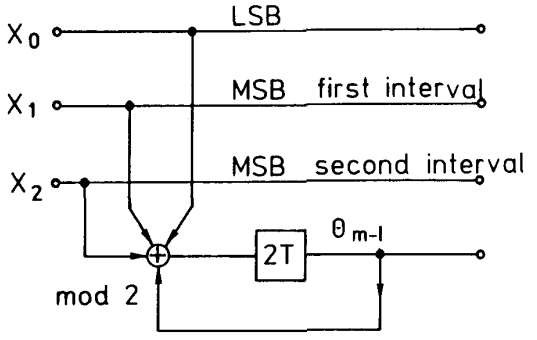

Fig. 4 The natural phase-state encoder for M=4, h=1/4, κ=2, μ=1

of MSK and each of them has an average probability 1/8. The signal-elements "x" represent the extension of MSK and each of them has an average probabilitity 1/16. The spectral power density of the 8-ary scheme over 2T is symmetrical to the carrier frequency, because signal-elements on all four circles of Fig. 1 have equal probabilities. It is almost identical to that of uncoded 4-ary CPM, h = 1/4.

The unequal probabilities of the signal-elements offer improved synchronization capabilities for these 8-ary schemes, because already the square of the signal includes spectral lines in spite of the fourth power (|9|). The signal-elements at the output of a squarer can simply be represented by a doubling of angle and magnitude in Fig. 1; see Fig. 5. Now for two circles the center of mass is outside the origin and therefore discrete spectral lines arise (cf.|10,11|). (This fact again indicates the relationship to MSK. There is CNR-loss of about 6,5 dB compared to M = 2, h = 1/2 using a squarer loop synchronization.) For the reduced set of used signal-elements a smaller number of correlators at the receiver generates a sufficient statistic of the received signal (L = 1: 6 instead of 8; L = 2: 20 instead of 32, L = 3: 56 instead of 128).

Although Fig. 4 indicates that all three binary inputs of the 8-ary modulation scheme are equivalent, the mapping rule for a combination with rate 2/3 convolutional codes must be optimized, because the inputs generate the phase-increments in different ways and the Euclidean distance is a nonlinear function of the superimposed phase-increments. An encoder structure, which only protects a LSB, is not indicated here.

The best codes found are listed in table 1-3 by their obvious encoder structures together with the normalized Euclidean distance for schemes with frequency impulses of types 1REC, 2RC, 3RC (cf.|1|) at several ENNB. (In many cases other codes achieve the same Euclidean distance, too.) In these tables results of the combination of rate 1/2 codes to quaternary CPM (single trellis-coded) from |6, 12, 13| are given for comparison. Especially for schemes with small decoding effort the double trellis-coded schemes clearly outperform the single trellis-coded.

For frequency impulses 1REC an optimization of rate 2/4 codes was performed without the restriction of the redundant mapper. No code was found better than those of table 1.

The simulation results given in Fig. 7 and 8 show that an increased number of nearest neighbour error events is not a severe disadvantage of double trellis-coded CPM. (The simulations were performed up to 100 independent error events separated by at least 10 error free symbols.)

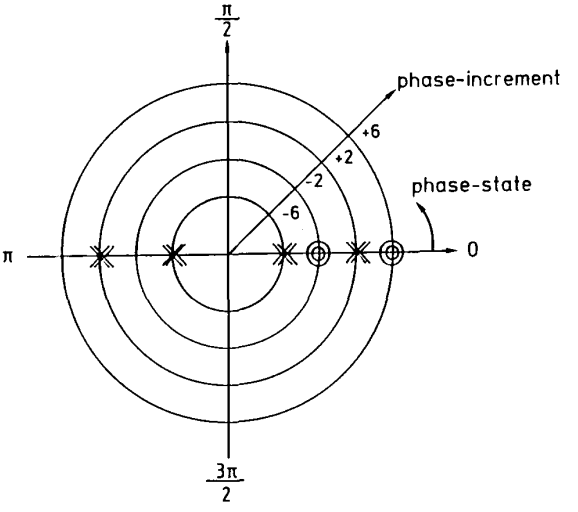

Fig. 5 representation of the squared signal-elements (M=4, h=1/4, κ=2, μ=1)

IV. REDUCED-STATE VITERBI-DECODING

In |8| it is shown that by the usage of a code with a longer constraint length combined with a suboptimum decoding algorithm a higher utilizable Euclidean distance d'_{min} may be achieved than by a shorter code and Maximum-Likelihood-Sequence-Estimation (MLSE) at the same ENNB. In almost all examples the best results were obtained by Decision-Feedback-Sequence-Estimation (DFSE |7|) with a state-reduction factor 2.

DFSE only is applicable, if the combined encoder-modulator trellis has a butterfly structure; i.e. the set of different states can be partitioned into classes, each of them comprising $2^{\kappa k}$ states with the property that all $2^{2\kappa k}$ branches of one class lead to exactly $2^{\kappa k}$ successor states. (Therefore no other branches reach any of these successor states.) Additionally all paths, which pass through states of one class will merge at the next step for each encoder input symbol.

From the linearity in GF (2) of the phase-state-encoder of the 8-ary modulation scheme for two intervals (Fig.4) the butterfly structure of the combined encoder modulation trellis can simply be proved. If frequency impulses with intersymbol-interference (L>1) are used, the phase-state encoder has to be completed by a 8-ary shift register with (L-1) stages (cf.|6|). Thus, the combined encoder in all cases is linear. Therefore an equivalent obvious encoder exists with a memory structure consisting of $\kappa \cdot k$ binary shift registers and without feedback |14|. But a shift register memory always has a trellis with butterfly structure which allows a state reduction by DFSE at any level (|7|,|8|).

This equivalent nonrecursive encoder demonstrates that in the combined encoder 2(L-1) binary delay elements are sufficient for a description of the ISI of the frequency impulses instead of 3(L-1); L>2. L=2 is a special case, as for the input x_1 (MSB of the first modulation interval) no delay-element must be provided within the natural encoder of the 2-fold scheme. Therefore some special conditions on the convolutional encoder exist for a common usage of delay elements by both encoders (|6|). All codes given in table 2 satisfy these conditions.

By the DFSE-Algorithm at a reduction level one (|7|) all states of a class are regarded as one hyperstate (see Fig. 6). The signal-element associate with a branch in the trellis of hyperstates is a function of the substate within the hyperstate, from which the branch emerges. The actual substate is uniquely determined by the branch, which leads to a hyperstate. Because a final decision has to be made between two paths, which enter the common hyperstate, the contribution of the last step

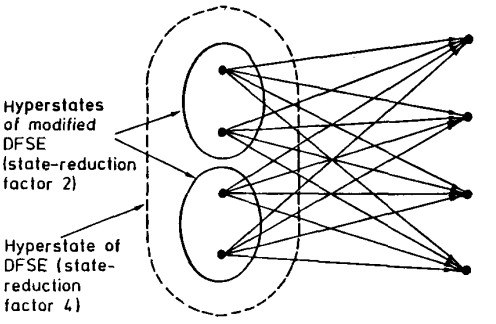

Fig. 6 State-combination to hyperstates for DFSE and modified DFSE

before the merge to their Euclidean distance is lost.

The normalized squared Euclidean distances utilizable by DFSE of the optimum codes are listed in table 1-3. Since κk=2 for these examples DFSE provides a state reduction of factor r_f=4.

For comparison results from |8| are given in the tables for the application of DFSE to single trellis-coded schemes (reduction factor r_f=2). Looking from the view point "minimal Euclidean distance" the double trellis-coded schemes with DFSE (r_f=4) clearly outperform schemes with MLSE and DFSE for single trellis-coded schemes.

The error propagation due to DFSE was studied by simulation; some results are given in Fig. 7 and 8. In contrast to the application of DFSE to single trellis-coded binary schemes (|8|) error propagation now is a slight problem. The simulation results are in contrast to the minimum Euclidean distances because each error event consists of more errors (cf. Fig. 8, 9). The reason for this problem is that now 4-ary symbols are stored in the decision-feedback-register, and therefore the probability of a right successiv decision after an error is less than for binary feedback. To overcome this problem we propose a slightly modified DFSE-algorithm:

A state reduction of a factor r_f=2 is achieved if only pairs of states of a 4-ary butterfly are combined into a hyperstate as shown in Fig.6. In spite of the quaternary input symbol a binary decision-feedback with less error propagation is sufficient for the specification of the substate. The code optimization for this modified DFSE includes an optimization, which pairs of states for each butterfly form the hyperstates. For L ≧ 2 this optimization always yields that such states are combined, from which branches emerge with associate signal-elements, which are identical within the second modulation interval. Fortunatelly in many cases these combinations of states to hyperstates can be done in such way that the distance losses does not affect minimal distance error events.

Therefore the number of states often can be reduced by a factor 2 without any loss of utilizable minimal Euclidean distance. In most examples the modified DFSE achieves the highest minimal distances (column r_f=2 in tables 1-3) at a given ENNB with the optimum code for MLSE of the next row.

The double trellis-coded schemes with modified DFSE not only have the best distances, but also show the best performance in the simulation results. The examples given in Fig. 7 and 8 demonstrate that the state reduction of factor 2 has quite no prize in bit error rate or number of errors per error event. Error propagation due to the binary decision-feedback almost is negligible. (It should be mentioned that this state-reduction without any losses also can be applied to uncoded M ≧ 4-ary CPM.)

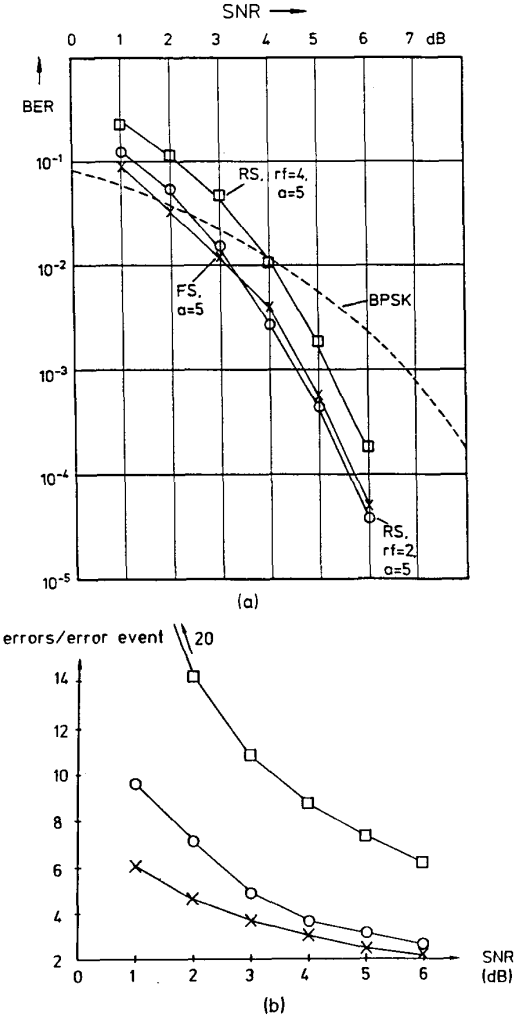

Fig. 7 Simulation results of the double trellis coded CPM (M=4, h=1/4, 1REC), at several SNR (dB). - (a) bit error rate; (b) errors per error event.

V. CONCLUSION

By the redundant mapping introduced in section II double trellis-coded CPM schemes can be constructed with very low numbers of trellis branches per symbol interval, which have to be processed by a Viterbi-decoder. These schemes not only outperform comparable single trellis-coded, but also offer improved receiver implementation properties (synchronization and correlators). By the application of a modified DFSE-algorithm the number of states may be halved in many cases without losses. Especially for smoothed frequency impulses (e.g. 2RC, 3RC) these methods allow a decrease of trellis branches per symbol interval by factors up to 8 compared to quaternary CPM combined with rate 1/2 convolutional codes without significant performance losses.

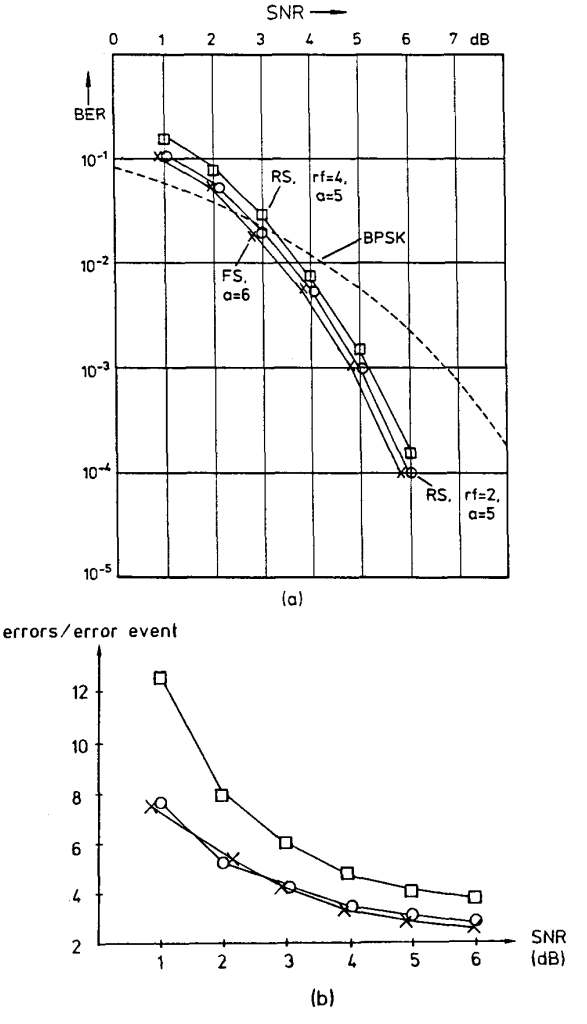

Fig. 8 Simulation results for frequency impulse 3RC. - (a) bit error rate; (b) errors per error event

REFERENCES

|1| J.B. Anderson, T. Aulin, C-E. Sundberg, Digital Phase Modulation, Plenum Press, New York, 1986.

|2| C-E. Sundberg, "Continuous Phase Modulation", IEEE Commun. Magazine, vol. 24, no. 4, pp. 25-38, April 1986.

|3| G. Ungerboeck, "Trellis-Coded Modulation with Redundant Signal Sets - Part I and II", IEEE Commun. Magazine, vol . 25, no. 2, pp. 5-21, Feb. 1987.

|4| D. Divsalar, M.K. Simon, "Multiple Trellis Coded Modulation (MTCM)", in Proc. GLOBECOM '86, vol. 2, pp. 30.8.1-30.8.7, Houston, Dez. 1986.

|5| L.-F. Wei, "Trellis-Coded Modulation with Multidimensional Constellations", IEEE Trans. Inform. Theory, vol. IT-33, no. 4, pp. 483-501, July 1987.

|6| J. Huber, W.L. Liu, "Convolutional Codes for CPM Using the Memory of the Modulation Process", in Proc. GLOBECOM '87, vol. 3, pp.43.1.1 - 43.1.5, Tokyo, Nov. 1987.

|7| M.V. Eyuboglu, S.U. Qureshi, "Reduced-State Sequence Estimation with Set Partitioning and Decision Feedback", in Proc. GLOBECOM '86, vol. 2, pp. 29.2.1-29.2.6, Houston, Dez. 1986.

|8| J. Huber, W.L. Liu, "Reduced-State-Viterbi-Detection of CPM Combined with Convolutional Codes", in Proc. SITA '87, vol. 2, pp. ED 2-2-1 - ED 2-2-6, Enoshima, Japan, Nov. 1987.

|9| T. Aulin and C-E. Sundberg, "Synchronization Properties of Continuous Phase Modulation", in Proc. GLOBECOM '82, Miami, Florida, USA, pp. D7.1.1-D7.1.7, Nov. 1982.

|10| W.C. Lindsey, M.K. Simon, Telecommunications Systems Engineering, Prentice-Hall, Englewood, N.Y., 1973.

|11| H. Beckmann, J. Huber, "Mittleres Leistungsspektrum gedächtnisbehafteter, digitaler Signalquellen", ntz Archiv, Bd. 10 (1988), H.2, pp. 45-54.

|12| G. Lindell, C-E. Sundberg, T. Aulin, "Minimum Euclidean Distance for Combination of Short Rate 1/2 Convolutional Codes and CPFSK Modulation", IEEE Trans. Inform. Theory, vol. IT-30, pp. 509-519, May 1984.

|13| S.V. Pizzi, S.G. Wilson, "Convolutional Coding Combined with Continuous Phase Modulation", IEEE Trans. Commun., vol. COM-33, pp. 20-29, Jan. 1985.

|14| G.D. Forney, "Convolutional Codes I: Algebraic Structure", IEEE Trans. Inform. Theory, vol. IT-16, pp. 720-738, Nov. 1970.

a	single trellis $r_c=1/2$ FS d^2_{min}	single trellis $r_c=1/2$ RS $r_f=2$ d'^2_{min}	double trellis $r_c=2/3$ FS d^2_{min} encoder $(x_0\ x_1\ x_2)$	RS $r_f=2$ d'^2_{min} encoder $(x_0\ x_1\ x_2)$	RS $r_f=4$ d'^2_{min} encoder $(x_0\ x_1\ x_2)$
1	—	—	———	———	1.15 $\begin{pmatrix}0&1&1+D\\1&0&0\end{pmatrix}$
2	—	—	———	2.73 cf. FS, a=3	2.73 $\begin{pmatrix}0&1&0\\D&0&1+D^2\end{pmatrix}$
3	0.73	2.64	2.73 $\begin{pmatrix}0&1&0\\D&0&1\end{pmatrix}$	3.88 cf. FS, a=4	3.30 $\begin{pmatrix}D&1+D&1+D\\1&1&1+D^2\end{pmatrix}$
4	3.00	3.42	4.00 $\begin{pmatrix}D&1+D^2&0\\0&0&1\end{pmatrix}$	4.18 $\begin{pmatrix}0&1+D+D^2&1+D^2\\1&0&D\end{pmatrix}$	4.15* $\begin{pmatrix}1+D&1+D&1\\D+D^2&1&1+D+D^2+D^3\end{pmatrix}$
5	4.42	4.24	4.88 $\begin{pmatrix}0&1+D+D^2&1\\1&D&D\end{pmatrix}$	4.75* $\begin{pmatrix}D&1+D&1+D\\D&1+D^2+D^3&D\end{pmatrix}$	
6	5.24	5.15	5.45* $\begin{pmatrix}D&1+D&D+D^2\\D+D^2&1&1+D^2+D^3\end{pmatrix}$		

Table 1: Optimum codes and squared normalized minimum Euclidean distances with FS- VA and RS-VA (M=4, h=1/4, 1REC)
* Search not complete

a	single trellis $r_c=1/2$ FS d^2_{min}	single trellis $r_c=1/2$ RS $r_f=2$ d'^2_{min}	double trellis $r_c=2/3$ FS d^2_{min} encoder $(x_0\ x_1\ x_2)$	RS $r_f=2$ d'^2_{min} encoder $(x_0\ x_1\ x_2)$	RS $r_f=4$ d'^2_{min} encoder $(x_0\ x_1\ x_2)$
2	—	—	———	———	2.00 cf. FS, a=4
3	—	0.61	———	2.60 cf. FS, a=4	2.98 $\begin{pmatrix}D&1+D^2&0\\0&0&1\end{pmatrix}$
4	0.66	2.93	2.65 $\begin{pmatrix}0&1&0\\D&0&1\end{pmatrix}$	4.00 cf. FS, a=5	3.66 $\begin{pmatrix}D^2&1+D+D^2+D^3&0\\0&0&1\end{pmatrix}$
5	2.98	3.92	4.00 $\begin{pmatrix}0&1&0\\D&0&1+D^2\end{pmatrix}$	4.52 $\begin{pmatrix}0&1&1+D+D^2\\1&1+D&1+D\end{pmatrix}$	4.34* $\begin{pmatrix}0&1+D^2&1\\D^2&D&1+D\end{pmatrix}$
6	4.12	4.73	4.57 $\begin{pmatrix}0&1&1+D\\1&D^2&D^2\end{pmatrix}$		

Table 2: Optimum codes and squared normalized minimum Euclidean distances with FS-VA and RS-VA (M=4, h=1/4, 2RC)

a	single trellis $r_c=1/2$ FS d^2_{min}	single trellis $r_c=1/2$ RS $r_f=2$ d'^2_{min}	double trellis $r_c=2/3$ FS d^2_{min} encoder $(x_0\ x_1\ x_2)$	RS $r_f=2$ d'^2_{min} encoder $(x_0\ x_1\ x_2)$	RS $r_f=4$ d'^2_{min} encoder $(x_0\ x_1\ x_2)$
3	—	—	———	———	2.16 cf. FS, a=5
4	—	0.47	———	2.42 cf. FS, a=5	2.88 $\begin{pmatrix}D&1+D^2&1\\0&0&1\end{pmatrix}$
5	0.48	2.85	2.42 $\begin{pmatrix}0&1&0\\D&0&1\end{pmatrix}$	3.40 cf. FS, a=6	3.46 $\begin{pmatrix}0&1&0\\D^2&0&1+D+D^2+D^3\end{pmatrix}$
6	2.86	3.06	3.40 $\begin{pmatrix}0&1&0\\D&0&1+D^2\end{pmatrix}$	4.00 cf. FS, a=7	
7	3.07	3.54	4.00 $\begin{pmatrix}D&1+D^2+D^3&0\\0&0&1\end{pmatrix}$		

Table 3: Optimum codes and squared normalized minimum Euclidean distances with FS-VA and RS-VA (M=4, h=1/4, 3RC)